Lithium–Air Battery

Deutsche Ausgabe: DOI: 10.1002/ange.201502039
Internationale Ausgabe: DOI: 10.1002/anie.201502039

Direct Detection of the Superoxide Anion as a Stable Intermediate in the Electroreduction of Oxygen in a Non-Aqueous Electrolyte Containing Phenol as a Proton Source**

Zhangquan Peng, Yuhui Chen, Peter G. Bruce, and Ye Xu**

Abstract: *The non-aqueous Li–air (O_2) battery has attracted intensive interest because it can potentially store far more energy than today's batteries. Presently Li–O_2 batteries suffer from parasitic reactions owing to impurities, found in almost all non-aqueous electrolytes. Impurities include residual protons and protic compounds that can react with oxygen species, such as the superoxide (O_2^-), a reactive, one-electron reduction product of oxygen. To avoid the parasitic reactions, it is crucial to have a fundamental understanding of the conditions under which reactive oxygen species are generated in non-aqueous electrolytes. Herein we report an in situ spectroscopic study of oxygen reduction on gold in a dimethyl sulfoxide electrolyte containing phenol as a proton source. It is shown directly that O_2^-, not HO_2, is the first stable intermediate during the oxygen reduction process to hydrogen peroxide. The unusual stability of O_2^- is explained using density functional theory (DFT) calculations.*

The electrochemical oxygen-reduction reaction (ORR) is at the heart of energy conversion and storage technologies including fuel cells and metal–air batteries.[1–3] However, the mechanism of the ORR, including the rate-limiting step, remains disputed even for the seemingly simple case of O_2 electro-reduction on Pt(111) in acidic solutions.[4] The Li version of the ORR, which is the key cathodic reaction of a Li–air (O_2) battery, is still less-well understood particularly in non-aqueous media owing to the formation of solid products that can easily obscure the interpretation of experimental results.[5,6]

To date much effort has been devoted to the investigation of the main reactions of Li–O_2 batteries, that is, the formation/decomposition of Li_2O_2. Much less attention has been paid to the potential parasitic reactions arising from the presence of minor amounts of impurities, such as protons and proton-containing compounds, which exist in almost all non-aqueous electrolytes. They can compete with Li^+ ions for the reduced oxygen species, such as superoxide anions[7] and drastically degrade the performance of the Li–O_2 cells. To eliminate or alleviate the parasitic reactions to an acceptable extent, it is crucial to have a fundamental understanding of these reactions.

Very few ORR studies have made conclusive identification of the reactive superoxide state (O_2^-) in protic media. Gewirth and Li reported O_2^- at 1165 cm^{-1} in ORR on Bi-modified Au surfaces in 0.1M $HClO_4$ by in situ surface enhanced Raman spectroscopy (SERS).[8] Using in situ surface enhanced infrared reflection absorption spectroscopy configured with attenuated total reflection (ATR-SEIRAS), Shao et al. reported a band at 1005-1016 cm^{-1} with O_2^- on a Pt electrode in 0.1M $NaClO_4$ + NaOH;[9] however, neither O_2^- nor HO_2 but only hydroperoxide ion (HO_2^-) was observed on an Au thin film electrode in 0.1M of either $HClO_4$ or $NaClO_4$.[10] Recently, Peng et al. reported direct evidence using in situ SERS that O_2 is first reduced to O_2^- in acetonitrile-based Li^+-containing electrolytes, which then forms LiO_2 on the electrode surface and disproportionates to Li_2O_2.[11]

Herein we report the direct detection of two surface species, O_2^- and hydrogen peroxide (H_2O_2), together in an in situ SERS study of the electrochemical ORR on a polycrystalline gold electrode under protic but non-hydroxylic conditions, by using an O_2-saturated solution of dry dimethyl sulfoxide (DMSO) containing tetrabutylammonium perchlorate ($TBAClO_4$) as the supporting salt, and phenol ($pKa = 18.0$) as the proton source (additional details of the electrochemical and SERS experiments can be found in Supporting Information). Our finding represents a departure from the commonly accepted ORR mechanism involving HO_2 as the first reduction intermediate in protic electrolytes. A reaction pathway is proposed, based on density functional theory (DFT) calculated energetics, to explain O_2 reduction to O_2^- and then to H_2O_2 under the experimental conditions. Although many experimental[8–10,12–14] and theoretical[15–19] studies of the ORR have been conducted on metal electrodes including Au and Pt, to our knowledge, the in situ spectroscopic detection of these two species simultaneously in the

[*] Prof. Z. Peng
State Key Laboratory of Electroanalytical Chemistry
Changchun Institute of Applied Chemistry
Chinese Academy of Sciences
Changchun, Jilin, 130022 (P.R. China)
E-mail: zqpeng@ciac.ac.cn
Dr. Y. Chen, Prof. P. G. Bruce
Department of Materials, University of Oxford
Oxford OX1 3PH (UK)
Prof. Y. Xu
Department of Chemical Engineering
Louisiana State University
Baton Rouge, LA 70803 (USA)
E-mail: yexu@lsu.edu

[**] Z.P. is indebted to the "Strategic Priority Research Program" of the CAS (Grant No. XDA09010401) and the "Recruitment Program of Global Youth Experts" of China. Theoretical work at LSU was supported in part by the U.S. NSF (under EPSCoR Cooperative Agreement EPS-1003897 with additional support from the Louisiana Board of Regents) and used high-performance computing resources provided by LSU.

Supporting information for this article is available on the WWW under http://dx.doi.org/10.1002/anie.201502039.

 © 2015 Wiley-VCH Verlag GmbH & Co. KGaA, Weinheim

same ORR system in proton source-containing media, and the use of DFT calculations to determine the electrochemical stability of O_2^- versus protonated O_2 species on a metal surface, have not been reported before.

The cyclic voltammograms at a macro Au disk electrode (diameter 2 mm) and the polarization curves at a micro Au disk electrode (diameter 25 μm) for the reduction of O_2 in DMSO before and after the addition of 20 mM phenol are shown in Figure 1 a,b, respectively. In the cyclic voltammetric (CV) experiments (Figure 1 a), the O_2/O_2^- wave lost its

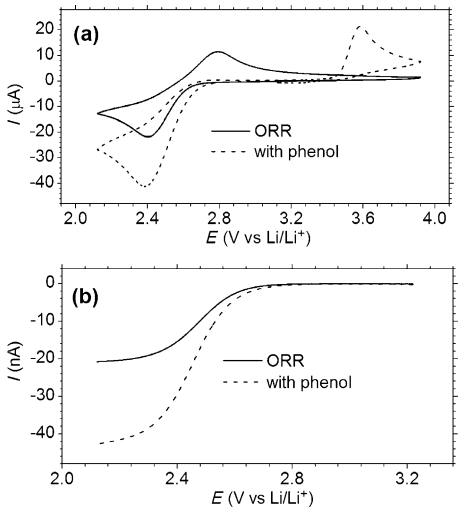

Figure 1. a) Cyclic voltammograms at a macro Au electrode (diameter 2 mm) and b) potential polarization at a micro Au electrode (diameter 25 μm) for ORR in the absence (solid line) and presence (dashed line) of phenol. Electrolyte solution is O_2-saturated DMSO containing 100 mM $TBAClO_4$, without and with 20 mM phenol. Potential scan rates are 0.1 Vs^{-1} and 5 mVs^{-1} for macro and micro Au electrodes, respectively.

reversibility and increased in height, with the number of electron transferred changing from $1e^-$ to $2e^-$ per O_2. The irreversible anodic wave observed at more positive electrode potential was related to the oxidation of phenate ions.[20] The transition of the O_2 reduction from $1e^-$ to $2e^-$ is further supported by the potential polarization experiment on an Au microelectrode, in which the limiting current was doubled when phenol was added (Figure 1 b).

The effect of added phenol on the O_2/O_2^- process in DMSO has been studied by Andrieux et al. on carbon electrodes,[20] and the following $2e^-$ reaction mechanism was proposed without spectroscopic identification of the reaction intermediates [Eq. (1)–(3)]:

$$O_2 + e^- \rightarrow O_2^- \quad (1)$$

$$O_2^- + PhOH \rightarrow HO_2 + PhO^- \quad (2)$$

$$HO_2 + O_2^- \rightarrow HO_2^- + O_2 \quad (3)$$

in which O_2^- and HO_2 are the proposed intermediates and these two species react with each other to form HO_2^-. To identify the intermediates in this ORR on Au electrodes, we performed in situ SERS experiments.

The SERS spectra were first recorded for O_2-saturated 0.1 M $TBAClO_4$ DMSO on a Au electrode before the addition of phenol. As can be seen in Figure 2 left panel, above 2.7 V

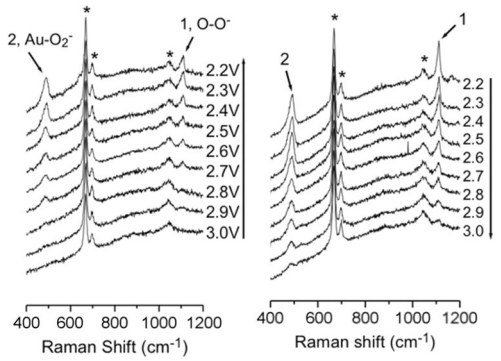

Figure 2. In situ SERS of ORR on a polycrystalline Au electrode in O_2-saturated DMSO containing 100 mM $TBAClO_4$ but no phenol. Left: The cathodic sweep from 3.0 to 2.2 V (vs. Li/Li^+). Right: the corresponding anodic sweep. Peaks marked with asterisks (*) are assigned to DMSO solvent.

(vs. Li/Li^+), that is, at potentials where no ORR takes place, the prominent peaks at 670, 700, and 1050 cm^{-1} (marked with asterisks, *) are associated with DMSO solvents. When the electrode potential was swept below 2.7 V at which ORR starts, a pair of new peaks at 1110 and 488 cm^{-1} ("1" and "2" in Figure 2, left panel) began to appear and grew in intensity with decreasing potential. We assign the 1110 cm^{-1} peak to the O–O stretching (ν_{O-O}) and the 488 cm^{-1} peak to the Au-O_2 stretching of O_2^- adsorbed on Au. This assignment is consistent with our report on ORR in acetonitrile,[11] the ν_{O-O} band of alkali-metal superoxide molecules,[21] and the measured ν_{O-O} of O_2^- radical solvated in water.[22] When the electrode potential was reversed, these two peaks gradually decreased and disappeared, indicating the reversibility of the redox couple of O_2/O_2^- (Figure 2, right panel). No solvent decomposition products were detected.

When phenol as the proton source was introduced in the experiment, the ORR changed from a $1e^-$ to a $2e^-$ process as the voltammetric measurements indicated (Figure 1). Interestingly, the 1110 and 488 cm^{-1} peaks identified with O_2^- remained almost unchanged, indicating O_2^- formation again. In addition, a new peak at 876 cm^{-1} ("3" in Figure 3, left panel) appeared at 2.5 V. It is assigned to the ν_{O-O} of H_2O_2.[19,23] For comparison, the stretching frequency of bulk metal-bound HO_2 is identified in 815–830 cm^{-1} using Raman spectroscopy,[24,25] suggesting that none of the peaks "1," "2," and "3" was due to HO_2. The absence of the H_2O_2 signals in the approximate range 2.5–2.7 V during the cathodic sweep (Figure 3, left panel) suggests that any further reduction process in this potential range occurs in the electrolyte via the solution-mediated reaction mechanism proposed by Andrieux et al.,[20] that is, forming HO_2 species in the electrolyte, with little if any H_2O_2 diffusing back to the electrode within the limited time span of the experiment to be

 © 2015 Wiley-VCH Verlag GmbH & Co. KGaA, Weinheim

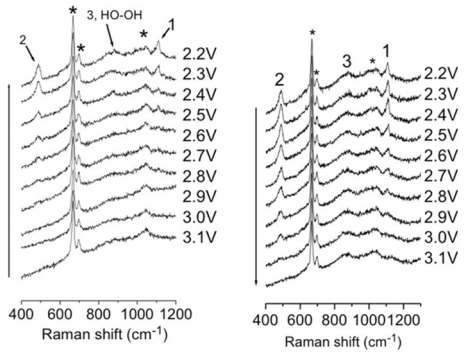

Figure 3. In situ SERS of ORR on a polycrystalline Au electrode in O_2-saturated DMSO containing 100 mM $TBAClO_4$ and 20 mM phenol. Left: The cathodic sweep from 3.1 to 2.2 V (vs. Li/Li^+) and Right: the corresponding anodic sweep.

seen in SERS. The reaction mechanism likely changes to a surface-mediated one below 2.5 V leading to significant H_2O_2 production, an issue that will be further addressed in the context of the DFT calculations below. When the potential was swept back to 3.1 V (Figure 3, right panel), the signals of O_2^- (peaks "1" and "2") gradually disappeared and only the signal of H_2O_2 (peak "3") remained. No hydrogen evolution occurred in the range of potentials in Figure 3. Recently, water, an ubiquitous proton source in even carefully dried organic electrolytes for non-aqueous Li–O_2 cells, has been suggested to play a key role in enabling redox shuttling mechanisms through electrolytes in Li ORR and Li_2O_2 electro-oxidation reactions.[26,27] We have verified that water was not involved, either as a contaminant in the solvent or as a product of the ORR, in our experiments.

To shed light on the nature of the surface oxygen species and the ORR mechanism in the phenol/DMSO electrolyte, the properties of O_2, HO_2, and H_2O_2 adsorbed (indicated by *) on DMSO/Au(111) have been calculated using periodic DFT implemented in VASP[28] (see Supporting Information for details of the theoretical methods). Their properties are listed in Table S1 in the Supporting Information and snapshots are shown in Figure 4. The DMSO interface (Figure 4a) stabilizes HO_2 (Figure 4c) and H_2O_2 (Figure 4d) compared to bare Au(111)[19] (see Table S1) in part through hydrogen bonding. The calculated ν_{O-O} of H_2O_2* is 893 cm^{-1}, which supports the assignment of the 876 cm^{-1} peak (peak "3" in Figure 3) to H_2O_2 in SERS. The calculated ν_{O-O} of HO_2* (see Table S1) is much lower, not higher, than that of H_2O_2*. While O_2 does not chemisorb on Au(111) in vacuo,[29,30] we find a spin-quenched stably adsorbed O_2 state in the top-bridge-top configuration on DMSO/Au(111) (Figure 4b). It has an O–O bond length of 1.325 Å, a Bader charge of −0.49, and ν_{O-O} of 1028 cm^{-1}. These characteristics identify it to be a superoxide state.

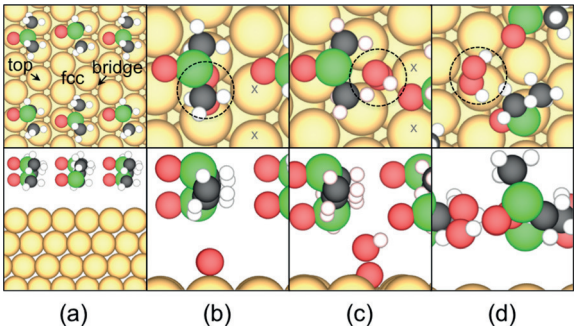

Figure 4. Top views (top panels) and side views (bottom panels) of DFT-optimized models for: a) DMSO/Au(111) interface with b) O_2, c) HO_2, and d) H_2O_2. Gold Au, red O, black C, and green S, white H atoms. O_2 states are circled in the top views. High-symmetry surface sites are labeled in (a). See Supporting Information for meaning of the "x" in (b, c).

The stability of HO_2* and H_2O_2* versus $O_{2(g)}$ as a function of the electrode potential is related to the standard hydrogen potential (SHE) by the computational hydrogen electrode (CHE).[15] The stability of O_2^-* versus $O_{2(g)}$ is related through the surface electrostatic potential of the O_2^-* state, to the absolute level of Li/Li^+[31] (see Supporting Information for details). The results (Figure 5) show that $O_{2(g)} + e^- + * \rightarrow O_2^-$* has an equilibrium potential of 2.88 V versus Li/Li^+ on

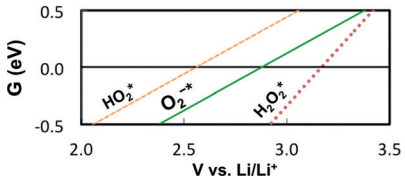

Figure 5. Free energy versus electrode-potential phase diagram for O_2 electro-reduction on Au(111) in protic, non-hydroxylic DMSO solution at pH 9.85. Zero on the *y*-axis represents gas-phase O_2 at room temperature and 0.1 bar.

Au(111) at the experiment conditions, in line with the onset potential of 2.7 V for O_2^- in the cathodic sweep, whereas $O_{2(g)} + H^+ + e^- + * \rightarrow HO_2$* is calculated to have an equilibrium potential of 2.56 V, lower than that of $O_{2(g)} + e^- + * \rightarrow O_2^-$*. Therefore, the first electron transfer produces a stable O_2^-* state instead of HO_2* on Au(111) owing to the low activity of H^+ in this system. A parallel situation exists in Li ORR on Au with O_2^- being the first intermediate, whereas LiO_2 is expected to form at lower potentials.[11,32,33] This interpolation scheme for the energetics of the O_2^-* does not apply to its other properties, such as the ν_{O-O} value. It can be expected that more-reducing conditions will lead to higher coverages of O_2^-* on the surface, which will cause the ν_{O-O} to blue-shift.[9]

We propose that O_2^-* is reduced to H_2O_2 on the Au electrode according to a modified version of the Andrieux mechanism [Eq. (4)–(6)]:

$$O_2 + e^- \rightarrow O_2^-* \quad (4)$$

$$O_2^-* + PhOH \rightarrow HO_2* + PhO^- \quad (5)$$

$$HO_2* + e^- + PhOH \rightarrow H_2O_2* + PhO^- \quad (6)$$

HO_2 is a necessary intermediate in this mechanism. It is easier for O_2^-* to transform to $O_{2(g)}$ instead of HO_2* above 2.56 V (in terms of calculated values). Below this potential

 © 2015 Wiley-VCH Verlag GmbH & Co. KGaA, Weinheim

HO_2* is stable versus $O_{2(g)}$ and so the surface-mediated mechanism becomes operative. This is consistent with the appearance of H_2O_2 at 2.5 V in the cathodic sweep, which suggests a change from a solution-mediated to surface-mediated mechanism at 2.5 V. HO_2* is calculated to be 0.32 eV less stable than O_2^-*, which constitutes a thermodynamic barrier to the formation of HO_2 in addition to any proton-transfer barrier that needs to be overcome, for the protonated species to appear. The combined barrier separating O_2^- and H_2O_2 thus accounts for the simultaneous presence of the two species on the Au electrode. Furthermore, the stability window of H_2O_2* versus $O_{2(g)}$ is calculated to extend up to 3.17 V, consistent with the fact that the H_2O_2 signals in SERS persist well above 2.5 V in the anodic sweep (Figure 3, right panel). It should be noted that the calculated results are subject to uncertainties in surface energetics, surface structural models, as well as the absolute level of the SHE, each on the order of around 0.1–0.2 eV.

In conclusion, by carrying out electrochemical ORR experiments under a non-aqueous but proton-containing environment on a polycrystalline Au electrode, and by performing detailed in situ SERS and DFT calculations, we have demonstrated for the first time that O_2^- and H_2O_2 can appear together in the same ORR system, providing direct evidence that the ORR can begin with $1e^-$ transfer to O_2 without coupled proton transfer even in the presence of a proton source. The phenol/DMSO electrolyte creates a sufficiently large potential window for O_2^- to be more stable than HO_2 and to be observable. Our findings show that the ORR mechanism depends intimately on the electrolyte composition and contribute new insights to the mechanistic understanding for this reaction which is of fundamental importance in electrochemical energy conversion and storage technologies.

Keywords: density functional theory calculations · Li–air batteries · oxygen reduction reactions · Raman spectroscopy · superoxide anion

How to cite: *Angew. Chem. Int. Ed.* **2015**, *54*, 8165–8168
Angew. Chem. **2015**, *127*, 8283–8286

[1] K. Kinoshita, *Electrochemical Oxygen Technology*, Wiley, **1992**.
[2] M. R. Tarasevich, A. Sadkowski, E. Yeager, in *Comprehensive Treatise of Electrochemistry*, *Vol. 7* (Eds.: B. E. Conway, J. O. M. Bockris, E. Yeager), Plenum Press, **1983**.
[3] Z. Peng, S. A. Freunberger, Y. Chen, P. G. Bruce, *Science* **2012**, *337*, 563–566.
[4] R. R. Adzic in *Electrocatalysis* (Eds.: J. Lipkowski, P. N. Ross), Wiley-VCH, New York, **1998**, p. 197.
[5] C. O. Laoire, S. Mukerjee, K. M. Abraham, E. J. Plichta, M. A. Hendrickson, *J. Phys. Chem. C* **2009**, *113*, 20127–20134.
[6] P. G. Bruce, S. A. Freunberger, L. J. Hardwick, J.-M. Tarascon, *Nat. Mater.* **2012**, *11*, 19–29.
[7] V. S. Bryantsev, M. Blanco, *J. Phys. Chem. Lett.* **2011**, *2*, 379–383.
[8] X. Li, A. A. Gewirth, *J. Am. Chem. Soc.* **2005**, *127*, 5252–5260.
[9] M. H. Shao, P. Liu, R. R. Adzic, *J. Am. Chem. Soc.* **2006**, *128*, 7408–7409.
[10] M. H. Shao, R. R. Adzic, *J. Phys. Chem. B* **2005**, *109*, 16563–16566.
[11] Z. Peng, S. A. Freunberger, L. J. Hardwick, Y. Chen, V. Giordani, F. Bardé, P. Novák, D. Graham, J.-M. Tarascon, P. G. Bruce, *Angew. Chem. Int. Ed.* **2011**, *50*, 6351–6355; *Angew. Chem.* **2011**, *123*, 6475–6479.
[12] B. B. Blizanac, V. Stamenkovic, N. M. Markovic, *Z. Phys. Chem. (Muenchen Ger.)* **2007**, *221*, 1379–1391.
[13] V. Stamenkovic, B. S. Mun, K. J. J. Mayrhofer, P. N. Ross, N. M. Markovic, J. Rossmeisl, J. Greeley, J. K. Nørskov, *Angew. Chem. Int. Ed.* **2006**, *45*, 2897–2901; *Angew. Chem.* **2006**, *118*, 2963–2967.
[14] J. L. Zhang, M. B. Vukmirovic, Y. Xu, M. Mavrikakis, R. R. Adzic, *Angew. Chem. Int. Ed.* **2005**, *44*, 2132–2135; *Angew. Chem.* **2005**, *117*, 2170–2173.
[15] J. K. Nørskov, J. Rossmeisl, A. Logadottir, L. Lindqvist, J. R. Kitchin, T. Bligaard, H. Jonsson, *J. Phys. Chem. B* **2004**, *108*, 17886–17892.
[16] M. J. Janik, C. D. Taylor, M. Neurock, *J. Electrochem. Soc.* **2009**, *156*, B126–B135.
[17] Y. X. Wang, P. B. Balbuena, *J. Phys. Chem. B* **2005**, *109*, 14896–14907.
[18] M. P. Hyman, J. W. Medlin, *J. Phys. Chem. B* **2006**, *110*, 15338–15344.
[19] D. C. Ford, A. U. Nilekar, Y. Xu, M. Mavrikakis, *Surf. Sci.* **2010**, *604*, 1565–1575.
[20] C. P. Andrieux, P. Hapiot, J. M. Saveant, *J. Am. Chem. Soc.* **1987**, *109*, 3768–3775.
[21] L. Andrews, J.-T. Hwang, C. Trindle, *J. Phys. Chem.* **1973**, *77*, 1065–1073.
[22] I. Janik, G. N. R. Tripathi, *J. Chem. Phys.* **2013**, *139*, 014302.
[23] X. Li, D. Heryadi, A. A. Gewirth, *Langmuir* **2005**, *21*, 9251–9259.
[24] B. S. Yeo, S. L. Klaus, P. N. Ross, R. A. Mathies, A. T. Bell, *ChemPhysChem* **2010**, *11*, 1854–1857.
[25] G. S. Kanner, D. P. Butt, *J. Phys. Chem. B* **1998**, *102*, 9501–9507.
[26] S. Meini, S. Solchenbach, M. Piana, H. A. Gasteiger, *J. Electrochem. Soc.* **2014**, *161*, A1306–A1314.
[27] N. B. Aetukuri, B. D. McCloskey, J. M. García, L. E. Krupp, V. Viswanathan, A. C. Luntz, *Nat. Chem.* **2015**, *7*, 50–56.
[28] G. Kresse, J. Furthmüller, *Phys. Rev. B* **1996**, *54*, 11169–11186.
[29] N. D. S. Canning, D. Outka, R. J. Madix, *Surf. Sci.* **1984**, *141*, 240–254.
[30] Y. Xu, M. Mavrikakis, *J. Phys. Chem. B* **2003**, *107*, 9298–9307.
[31] E. Skúlason, G. S. Karlberg, J. Rossmeisl, T. Bligaard, J. Greeley, H. Jónsson, J. K. Nørskov, *Phys. Chem. Chem. Phys.* **2007**, *9*, 3241–3250.
[32] G. K. P. Dathar, W. A. Shelton, Y. Xu, *J. Phys. Chem. Lett.* **2012**, *3*, 891–895.
[33] Y. Xu, W. A. Shelton, *J. Chem. Phys.* **2010**, *133*, 024703.

Received: March 4, 2015
Published online: May 26, 2015

© 2015 Wiley-VCH Verlag GmbH & Co. KGaA, Weinheim